Mathematical Biosciences 245 (2013) 86–95

Contents lists available at SciVerse ScienceDirect

Mathematical Biosciences

journal homepage: www.elsevier.com/locate/mbs

Modeling human postural sway using an intermittent control and hemodynamic perturbations

Taishin Nomura [a,*], Shota Oshikawa [a], Yasuyuki Suzuki [a], Ken Kiyono [a], Pietro Morasso [b]

[a] Graduate School of Engineering Science, Osaka University, Toyonaka, Osaka 5608531, Japan
[b] Fondazione Istituto Italiano di Tecnologia, RBCS Department, Genoa, Italy

ARTICLE INFO

Article history:
Available online 19 February 2013

Keywords:
Postural sway
Posture control
Intermittent control
Power law
Hemodynamics
Noise

ABSTRACT

Ground reaction force during human quiet stance is modulated synchronously with the cardiac cycle through hemodynamics [1]. This almost periodic hemodynamic force induces a small disturbance torque to the ankle joint, which is considered as a source of endogenous perturbation that induces postural sway. Here we consider postural sway dynamics of an inverted pendulum model with an intermittent control strategy, in comparison with the traditional continuous-time feedback controller. We examine whether each control model can exhibit human-like postural sway, characterized by its power law behavior at the low frequency band 0.1–0.7 Hz, when it is weakly perturbed by periodic and/or random forcing mimicking the hemodynamic perturbation. We show that the continuous control model with typical feedback gain parameters hardly exhibits the human-like sway pattern, in contrast with the intermittent control model. Further analyses suggest that deterministic, including chaotic, slow oscillations that characterize the intermittent control strategy, together with the small hemodynamic perturbation, could be a possible mechanism for generating the postural sway.

1. Introduction

Human upright posture during quiet standing, as a mechanical system when no active neural control is provided, is unstable due to insufficient passive stiffness of the ankle joint for overcoming the gravitational toppling torque [2–4]. The instability is saddle type, involving both stable and unstable dynamic modes [2]. Those modes correspond to stable and unstable manifolds of the upright saddle point in the state space representation of the mechanical system [5]. The central nervous system stabilizes such unstable posture, using time-delayed neural feedback control mechanisms that generate the active control torque, in a robust way while maintaining flexibility that allows the standing body to exhibit measurable postural sway.

Amplitude of postural sway, measured as a fluctuating motion of the Center of Pressure (CoP) on the standing ground, in the anterior–posterior direction is about 0.02 m during quiet standing in healthy adults [6,7]. This means that the total ankle joint torque (sum of the passive and the active torques) varies with an amplitude of about 12 Nm for a subject with body weight of 600 N. Conforto et al. [1] showed that the ground reaction force during human quiet standing was modulated synchronously with the cardiac cycle through hemodynamics. In particular, amplitude of this almost periodic modulation in the anterior–posterior direction (shear force at soles) is about 0.3 N, implying that the corresponding amplitude of the hemodynamic momentum perturbation to the ankle joint is 0.3 N × 1.3 m∼0.4 Nm, where 1.3 m represents the distance between the heart, as the force-origin, and the ankle joint. Although this hemodynamic perturbation torque is only 3% of the total ankle joint torque, it is the most clearly identified and directly measured source of endogenous perturbation that possibly induces postural sway, among other sources such as respiration [8] and sensory noise [9]. Can this small hemodynamic perturbation be the major source of endogenous perturbation? If this is the case, a way of stabilizing the upright posture should be flexible and might be associated with bounded stability [10].

Collins and De Luca showed that postural sway for healthy adults exhibited power law behaviors [11]. They analyzed the mean square displacement of CoP time series data $x(t)$, defined as $< (x(t+\tau) - x(t))^2 > \sim \tau^{2H}$ where H is the scaling exponent, and showed that CoP sway exhibited three approximate scaling regions with $H \sim 4/5, H \sim 1/4$, and $H \sim 0$. They suggested that those exponents could be interpreted, respectively, as the following behaviors; (1) short-term region (over about 0.7 Hz) where $x(t)$ behaved as a positively correlated random walk corresponding to successive fallings due to the gravitational drift, (2) long-term region (about 0.1–0.7 Hz) where $x(t)$ behaved as a negatively correlated random walk corresponding to repulsive movements counteracting the falling movements, and (3) very-long-term

* Corresponding author. Tel.: +81 6 6850 6532; fax: +81 6 6850 6534.
E-mail address: taishin@bpe.es.osaka-u.ac.jp (T. Nomura).

0025-5564/$ - see front matter © 2013 Elsevier Inc. All rights reserved.
http://dx.doi.org/10.1016/j.mbs.2013.02.002

region (below about 0.1 Hz) where $x(t)$ is saturated. They also suggested that CoP sway might be better considered as a stochastic process rather than chaotic dynamics based on their analyses on the correlation dimension and the Lyapunov exponent. Note that the mean square displacement, known also as the two-point correlation function or the stabilogram diffusion plot of the CoP is just an alternative expression of the auto-correlation function of the CoP, which is the inverse Fourier transform of the power spectral density (PSD) of the CoP [12]. Thus, the three scaling regions appear also in the PSD of the CoP as $f^{-\beta}$ with f being the frequency, where the two types of scaling exponents are inter-related as $\beta = 2H + 1$ [13].

In this study, we consider postural sway dynamics of an inverted pendulum model with two different active neural control strategies; namely, the continuous-time stiffness control model [14] and the discontinuous-time (or intermittent) control model [5]. The use of these two models is motivated by the recent debates on whether the central nervous system utilizes continuous feedback controllers [15,14,16–18] or intermittent feedback controllers [19,10,5,20–25] for stabilizing the unstable posture. We examine whether each control model can exhibit human-like postural sway exhibiting the power law behavior in the presence of the hemodynamic perturbation. To this end, the hemodynamic perturbation is modeled simply by a periodic and/or a random forcing signal, in both cases with the small amplitude experimentally observed by [1].

In Section 2, we introduce the continuous and the intermittent control models, and describe their dynamics when no endogenous perturbation is applied. Mathematical methods to characterize dynamics of the models are also described. In particular, Poincaré maps that observe the state of the pendulum stroboscopically are defined, by which we examine how the dynamics and the power law behavior of the intermittent control model alter depending on the value of an important parameter of the model. We perform bifurcation analysis, Lyapunov exponent analysis, and spectral analysis for this aim. Section 3 describes results of the analyses. We show that the continuous control model with typical feedback gain parameters hardly exhibits the human-like sway pattern, while the intermittent control does. We discuss the results in Section 4.

2. Methods

2.1. A single inverted pendulum model

The human upright posture can be modeled by the motion of a single inverted pendulum as

$$I\ddot{\theta}(t) = mgh\theta(t) + T(t) \tag{1}$$

where I represents the moment of inertia of human body around the ankle, θ the tilt angle, g the gravity acceleration, m the body mass, h the distance from the ankle joint to the center of mass of the body, T the total ankle torque, and $mgh\theta$ the linearized gravitational toppling torque for small θ during quiet standing. Those parameter values are exactly the same as in [5]. The ankle joint torque T at time t is modeled as

$$T(t) = -K\theta(t) - B\dot{\theta}(t) + T_{\text{act}}(t) + T_{\text{dist}}(t). \tag{2}$$

The first two terms on the right-hand side represent passive feedback torques generated by the intrinsic mechanical impedance of the ankle joint (K and B are the passive stiffness and viscosity, respectively) with no time delay. The third term T_{act} represents the active neural feedback torque determined by the central nervous system as a function of delay-affected tilt angle $\theta_\Delta \equiv \theta(t-\Delta)$ and angular velocity $\omega_\Delta \equiv \omega(t-\Delta) \equiv \dot{\theta}(t-\Delta)$ with Δ being the feedback delay time due to the neural signal transmission. The last term T_{dist} is an endogenous, i.e. internal disturbance that is often modeled as a colored stochastic torque noise. The state space representation of Eq. (1) is as follows.

$$\frac{d}{dt}\begin{pmatrix}\theta\\ \omega\end{pmatrix} = \begin{pmatrix}0 & 1\\ \frac{mgh-K}{I} & -\frac{B}{I}\end{pmatrix}\begin{pmatrix}\theta\\ \omega\end{pmatrix} + \frac{1}{I}\begin{pmatrix}0\\ T_{\text{act}}\end{pmatrix} + \frac{1}{I}\begin{pmatrix}0\\ T_{\text{dist}}\end{pmatrix} \tag{3}$$

or formally

$$\frac{dx}{dt} = Ax + u(x_\Delta) + d \tag{4}$$

where $x = (\theta, \omega)^T$ and $x_\Delta = (\theta_\Delta, \omega_\Delta)^T$. The terms Ax, u, and d define the vector field of the non-actively-actuated mechanical system, the active feedback control vector, and the disturbance vector, respectively.

According to the experimental evaluations of the passive ankle visco-elasticity [3,4], we set as $K = 0.8mgh$ Nm/rad and $B = 4.0$ Nms/rad. Thus, $mgh - K > 0$, and the upright state $x = (0,0)^T$ is an unstable equilibrium of saddle type, with stable and unstable manifolds when no active control is provided, i.e. $u = 0$ [5]. For the body parameter values used here, the stable and unstable manifolds of $dx/dt = Ax$ on the θ-ω plane are given, respectively, by the straight lines passing through the origin;

$$\omega = \lambda^- \theta \sim -1.434\theta \tag{5}$$

and

$$\omega = \lambda^+ \theta \sim 1.367\theta \tag{6}$$

where

$$\lambda^\pm = \frac{1}{2}\left(-B/I \pm \sqrt{(B/I)^2 + 4(mgh-K)/I}\right). \tag{7}$$

2.2. Continuous and intermittent control models

We consider two different implementations of the delayed active feedback torque. One is the conventional proportional (P) and derivative (D) controller, referred to as the continuous controller that generates $T_{\text{act}}^{\text{cont}}$ [14]. The other is the intermittent controller, by which the PD feedback control is switched on and off, depending on the delayed state of the pendulum x_Δ [5]. The corresponding torque is referred to as $T_{\text{act}}^{\text{int}}$. For both cases, the feedback delay time is set as $\Delta = 0.2$ s according to the experimental evaluation by [26].

The continuous controller is defined as;

$$T_{\text{act}}^{\text{cont}}(t) = -P^{\text{cont}}\theta_\Delta - D^{\text{cont}}\omega_\Delta \tag{8}$$

where P^{cont} and D^{cont} are the P and D gains, respectively. Typical gain values that have been estimated by previous studies and also used in this study are $P^{\text{cont}} = 471$ Nm/rad, corresponding to $0.8mgh$, and $D^{\text{cont}} = 270$ Nms/rad [14]. The upright posture $x = 0$ is asymptotically stable of focus type for those values. Maurer et al. reported that human postural sway data were best fitted by those values with a given colored torque noise (see Discussion for the use of the colored random noise) [14]. The parameter point $(P^{\text{cont}}, D^{\text{cont}}) = (471, 270)$ is located almost in the middle of a narrow stability region in the P^{cont}-D^{cont} parameter plane. Such stability region is approximately represented by the following three inequalities: $P^{\text{cont}} > mgh - K, D^{\text{cont}} < I/\Delta$, and $D^{\text{cont}} > P^{\text{cont}}\Delta - B$ as shown in [5]. Fig. 1A shows transient dynamics of the continuous control model when $T_{\text{dist}} = 0$, where the model shows a rapid damping with oscillation of about 0.8 Hz.

The intermittent controller is defined as;

$$T_{\text{act}}^{\text{int}}(t) = \begin{cases} -P^{\text{int}}\theta_\Delta - D^{\text{int}}\omega_\Delta, & (\theta_\Delta, \omega_\Delta)^T \in S_{\text{on}} \\ 0, & (\theta_\Delta, \omega_\Delta)^T \in S_{\text{off}} \end{cases} \tag{9}$$

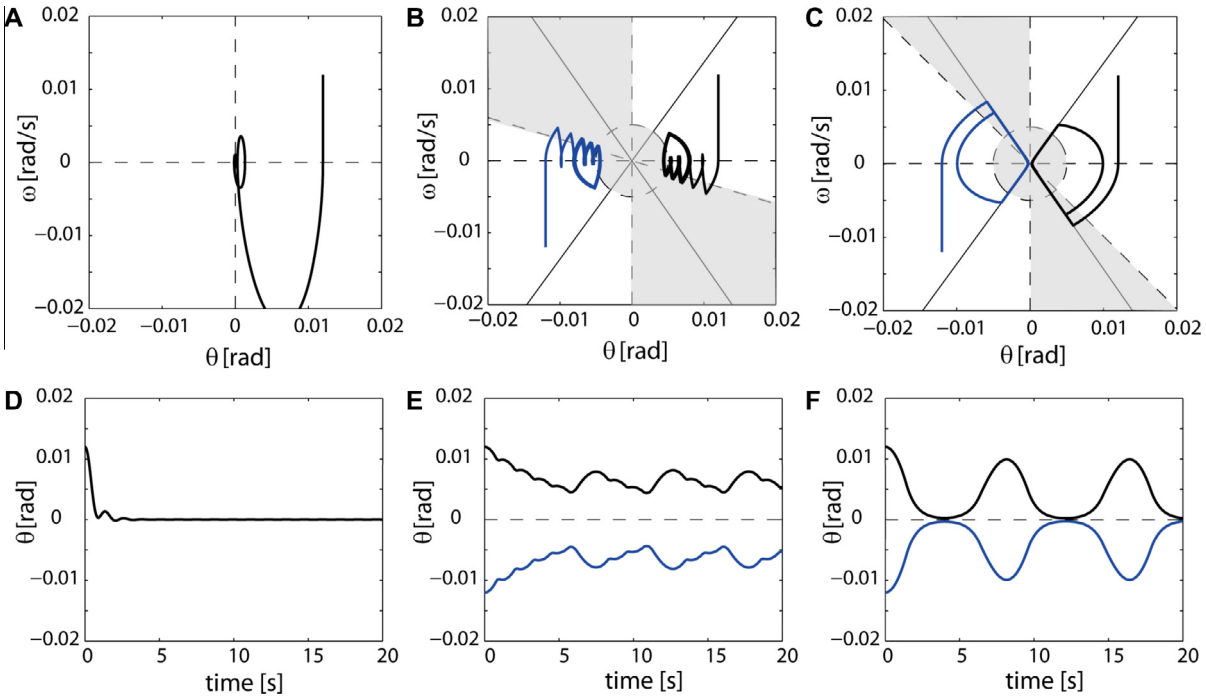

Fig. 1. Typical dynamics of the continuous and the intermittent control models without endogenous disturbance torque. A (and D): The continuous control model. B (and E) and C (and F): The intermittent control model with different parameter values of a that determines the slope of switching boundary line. a =-0.3 and −0.989 for B and C, respectively. In B and C, the gray area represents the off-region S_{off}, and the remaining white areas are the on-region S_{on}. See Eq. (9). In B and C, two trajectories starting from two different initial states. They asymptotes to different limit cycles that have symmetrical shapes with respect to the origin.

where S_{on} and S_{off} define the regions in the θ-ω plane, by which the state-dependent activation and inactivation of the active torque are determined (Figs. 1B and 1C). The PD feedback torque is actively generated when the delayed-state of the pendulum $x_\Delta = (\theta_\Delta, \omega_\Delta)^T$ is located in S_{on}, while no active torque is generated when x_Δ is in S_{off}. We consider these regions (on-region and off-region) according to [5], in which S_{on} and S_{off} are separated by the boundaries defined by $\theta_\Delta = 0, \dot{\theta}_\Delta = a\theta_\Delta$ and $\theta_\Delta^2 + \dot{\theta}_\Delta^2 = r^2$ (see Figs. 1B and 1C). The parameter r is fixed at 0.005 throughout the study, determining the circular sensory dead zone around the upright position. We consider various values of the parameter a, which determines the slope of the boundary line $\dot{\theta}_\Delta = a\theta_\Delta$, in the range of $[-1.4, 0]$. P^{int} and D^{int} are, respectively, the P and D gains of the intermittent controller when it is activated for $x_\Delta \in S_{\text{on}}$. The gains are set as $P^{\text{int}} = 147$ Nm/rad corresponding to $0.25mgh$ and $D^{\text{int}} = 10$ Nms/rad. Notice that these values are much smaller than P^{cont} and D^{cont}, providing a basis of flexible posture with a small joint impedance even when the active feedback control is turned on. However, this set of small parameter values is outside the stability region of the continuous control model, and thus, if the intermittent controller were activated permanently regardless of the pendulum's state, the upright equilibrium would be unstable of focus type due to the delay-induced instability. Despite the fact that upright equilibrium is also unstable of saddle type when the intermittent controller is permanently turned off, it is remarkable that a smart switching between the activation and the inactivation of the active controller can establish a bounded stability of the inverted pendulum [5].

Typical steady-state dynamics of the intermittent control model without disturbance is a periodic limit cycle solution (Figs. 1B and C.),[1] in which hyperbolic curved segments of the solution are governed by the saddle type vector field of $dx/dt = Ax$ without the active torque, and the remaining elliptic arc segments are by the unstable focus type vector field of $dx/dt = Ax + u(x_\Delta)$ with the active torque. The limit cycle solution for $a = -0.989$ (Fig. 1C) well illustrates features of the intermittent control model, in which the pendulum's state x just after the active torque is switched off is almost exactly on the stable manifold of the saddle point for $dx/dt = Ax$, resulting in the slow dynamics approaching the saddle point along the stable manifold, followed then by the slow falling away from the saddle point along the unstable manifold until x_Δ gets out the off-region S_{off}, leading to the slow oscillatory dynamics together with the unstable focus dynamics with the active torque that pulls the pendulum's state back to the stable manifold in the off-region. In Figs. 1B and C, two trajectories starting from two different initial states are depicted. They asymptotes to different limit cycles that have symmetrical shapes with respect to the origin, meaning that the intermittent control model shows bistability.

2.3. Models of endogenous disturbance

We consider three types of the disturbance torque T_{dist}. One is a periodic forcing $T_{\text{dist}}^{\text{per}}$ modeling the periodic component of the hemodynamics, by assuming simply that the heart beat is periodic. The second is a Gaussian white noise $T_{\text{dist}}^{\text{noise}}$ modeling the random component of hemodynamics. The third is the combination of $T_{\text{dist}}^{\text{per}}$ and $T_{\text{dist}}^{\text{noise}}$ as the total hemodynamic perturbation $T_{\text{dist}}^{\text{hemo}}$;

$$T_{\text{dist}}^{\text{per}}(t) = R\sin 2\pi f_{\text{hemo}} t \tag{10}$$

$$T_{\text{dist}}^{\text{noise}}(t) = \sigma\xi(t) \tag{11}$$

$$T_{\text{dist}}^{\text{hemo}}(t) = T_{\text{dist}}^{\text{per}} + T_{\text{dist}}^{\text{noise}} \tag{12}$$

where $\xi(t)$ is a standard Gaussian white noise with the expectation $E[\xi(t)] = 0$ and the auto-correlation $E[\xi(t)\xi(t+\tau)] = \delta(\tau)$. R and σ represent the amplitude of periodic and random components of the hemodynamic perturbation, respectively.

We examine the influence of those disturbances on both continuous and intermittent control models. The amplitude of periodic forcing R is fixed at 0.4 Nm, corresponding to the amplitude of

[1] All numerical simulations of the continuous and intermittent control models were performed using the forward Euler method with time step 0.001 s. See [5] for the integration of stochastic differential equations.

hemodynamic perturbation obtained by the time-locked average of the CoP sway data with respect to every R-wave of ECG [1]. The frequency of periodic forcing f_{hemo} is fixed at 1.2 Hz, corresponding to the typical heart beat frequency. The intensity of random noise $T_{\text{dist}}^{\text{noise}}$ is fixed at $\sigma = 0.09$ Nm, which corresponds to the standard deviation of the almost periodic hemodynamic perturbation to the ankle joint as obtained experimentally by Conforto et al. [1].

2.4. Poincaré maps, bifurcation and Lyapunov exponent analysis

Dynamics of the continuous and intermittent control models are analyzed using Poincaré maps. In particular, when the continuous and intermittent control models are forced by the periodic ($T_{\text{dist}}^{\text{per}}$) or the noisy periodic ($T_{\text{dist}}^{\text{hemo}}$) hemodynamic disturbance, the state of the pendulum (θ, ω) is observed stroboscopically (periodically) at every sinusoidal peak of $T_{\text{dist}}^{\text{per}}$, i.e. every $1/f_{\text{hemo}}$ s, to obtain a sequence of states of the pendulum $\{(\theta_n, \omega_n)\}$ with n being the observed cycle number. Dynamics of the observed states may be described by a stroboscopic Poincaré map as

$$(\theta_{n+1}, \omega_{n+1}) = F(\theta_n, \omega_n) \tag{13}$$

where $F : R^2 \to R^2$, which is parameterized by the noise intensity σ (and also the parameter a in the case of the intermittent control model). If $\sigma = 0$, it describes deterministic dynamics of the pendulum, otherwise stochastic. For example, if postural sway is simply entrained by (1:1 phase-locked to) the periodic forcing for $\sigma = 0$, we have a sequence of identical states, i.e., $(\theta_n, \omega_n) = (\theta_{n+1}, \omega_{n+1}) \equiv (\bar{\theta}, \bar{\omega})$ that satisfies $(\bar{\theta}, \bar{\omega}) = F(\bar{\theta}, \bar{\omega})$ as the steady state dynamics, where $(\bar{\theta}, \bar{\omega})$ is a fixed point of the map F. In the intermittent model, for some values of a, there might be cases in which $(\bar{\theta}, \bar{\omega}) = F^p(\bar{\theta}, \bar{\omega})$ holds for a positive integer p, where $(\bar{\theta}, \bar{\omega})$ is a fixed point of the map F^p, and it is also a p-periodic point of the map F, generating a repeated p-periodic sequence of $\{(\bar{\theta}, \bar{\omega}), F(\bar{\theta}, \bar{\omega}), \cdots, F^{p-1}(\bar{\theta}, \bar{\omega})\}$. Moreover, if the postural sway exhibits non-periodic dynamics in response to the periodic forcing for $\sigma = 0$, we have a non-periodic, possibly chaotic sequence of states.

The intermittent control model exhibits oscillatory dynamics even without the periodic hemodynamic forcing function, as shown in Figs. 1B and C. We analyzed such oscillatory postural sway using another type of Poincaré map as defined by [5], in which the boundary line $\dot{\theta}_\Delta = a\theta_\Delta$ is considered as a Poincaré section[2] Σ. We observed the state of the pendulum repeatedly when it gets across Σ in the direction of inactivating the active torque and we denote the corresponding map as follows:

$$(\theta_{n+1}, \omega_{n+1}) = G(\theta_n, \omega_n) \tag{14}$$

where $G : \Sigma \to \Sigma$ is parameterized by a and σ as in the map F. In Fig. 1B, for example, steady state limit cycle gets across the section Σ from the on-region to the off-region three times in one cycle, generating a repeated sequence of $\{(\bar{\theta}, \bar{\omega}), G(\bar{\theta}, \bar{\omega}), G^2(\bar{\theta}, \bar{\omega})\}$ as a 3-periodic point of the map G.

Postural sway dynamics of the intermittent control model changes depending on the parameter value of a. One can see differences in the shape of the limit cycle solutions for different values of a in Figs. 1B and 1C. The parameter a as the slope of switching boundary line determines the position of the pendulum's state immediately after the active control is switched off, after which the state point evolves according to the saddle-type vector field. In this study, we examine how the parameter value of a alters the postural sway dynamics by calculating a bifurcation diagram as a changes using the Poincaré maps of Eqs. (14) and (13). To this end, we simulated dynamics of the intermittent control model with and without hemodynamic forcing, and obtained sets of sequences $\{(\theta_n, \omega_n)\}$ for various values of a. In the bifurcation diagram, each sequence $\{\theta_n\}$ is plotted as the function of a. In the presence of the stochastic perturbation ($\sigma = 0.09$ Nm), the bifurcation diagram may become noisy, representing a stochastic bifurcation diagram [27,28].

The largest Lyapunov exponents are estimated using a method developed in [29,30] for both noise-less deterministic and noisy stochastic sway sequences $\{\theta_n\}$, by which we determine whether the sway dynamics of the model are chaotic.

2.5. Power spectral density of sway

Postural sway obtained by the continuous and the intermittent control models are characterized by the power spectral density (PSD) function. We are interested in finding values of the parameter a of the intermittent control model, for the deterministic ($\sigma = 0$ Nm/rad) and the stochastic ($\sigma = 0.09$ Nm/rad) cases, that can exhibit the power law behavior at the low frequency band 0.1–0.7 Hz. We estimated the PSD using FFT, and examined how the PSD shape changes as the function of a with and without the small random torque $T_{\text{dist}}^{\text{noise}}$.

The power law behavior at the long-term region was quantified by the slope of PSD at the low frequency band 0.1–0.7 Hz for the intermittent control model. The slope was obtained by least square linear regression. The absolute value of the slope represents the scaling exponent β, which is related to the other type of exponent H as $H = (\beta - 1)/2$. More specifically, $H \sim 1/4$ implies $\beta \sim 1.5$, as characterized by [11].

3. Results

3.1. Typical dynamics of the models with endogenous disturbance

Figs. 2–4 exemplify typical dynamics of the continuous and the intermittent control models when they are disturbed by the hemodynamic perturbation in the three different ways; namely, $T_{\text{dist}}^{\text{per}}$ with $f_{\text{hemo}} = 1.2$ Hz with no random component, $T_{\text{dist}}^{\text{noise}}$ with no periodic component, and $T_{\text{dist}}^{\text{hemo}}$ as the sum of both. The figures show how each component of the hemodynamic perturbation alters the model's dynamics in comparison with the corresponding dynamics with no disturbance in Figs. 1A, B and C.

3.1.1. Dynamics of the continuous model with endogenous disturbance

The continuous control model with typical values of the active feedback gains exhibits sway with a tiny amplitude for any of $T_{\text{dist}}^{\text{per}}$, $T_{\text{dist}}^{\text{noise}}$ and $T_{\text{dist}}^{\text{hemo}}$ (Fig. 2). In the case only with the periodic component, the pendulum oscillates simply with the forcing frequency f_{hemo}=1.2 Hz, and the PSD has a sharp peak at $f_{\text{hemo}} = 1.2$ Hz. When the continuous control model is driven by the random component $T_{\text{dist}}^{\text{noise}}$ or by the noisy periodic force $T_{\text{dist}}^{\text{hemo}}$, the pendulum fluctuates like a white noise of small intensity. The corresponding PSD shows a flat dependency on the frequency below 1.0 Hz including the low frequency band at 0.1–0.7 Hz. Indeed, the PSD of the continuous control model can be analytically calculated as

$$S(f) = \frac{\sigma^2}{\left|-4\pi^2 I f^2 + 2\pi i B f + K - mgh + e^{-2\pi i \Delta f}(P^{\text{cont}} + 2\pi i D^{\text{cont}} f)\right|^2} \tag{15}$$

which shows a good agreement with the numerically obtained PSD in Fig. 2H. The corner frequency f_c of the PSD can be approximated as

$$f_c \sim \frac{1}{2\pi}\sqrt{\frac{K + P^{\text{cont}} - mgh}{I - D^{\text{cont}}\Delta}} \tag{16}$$

[2] Rigorously speaking, the boundary line $\dot{\theta}_\Delta = a\theta_\Delta$ cannot be a Poincaré section, because there are trajectories that do not transverse the boundary line. Nevertheless, examining dynamics of the discrete state at every switching-off event is useful.

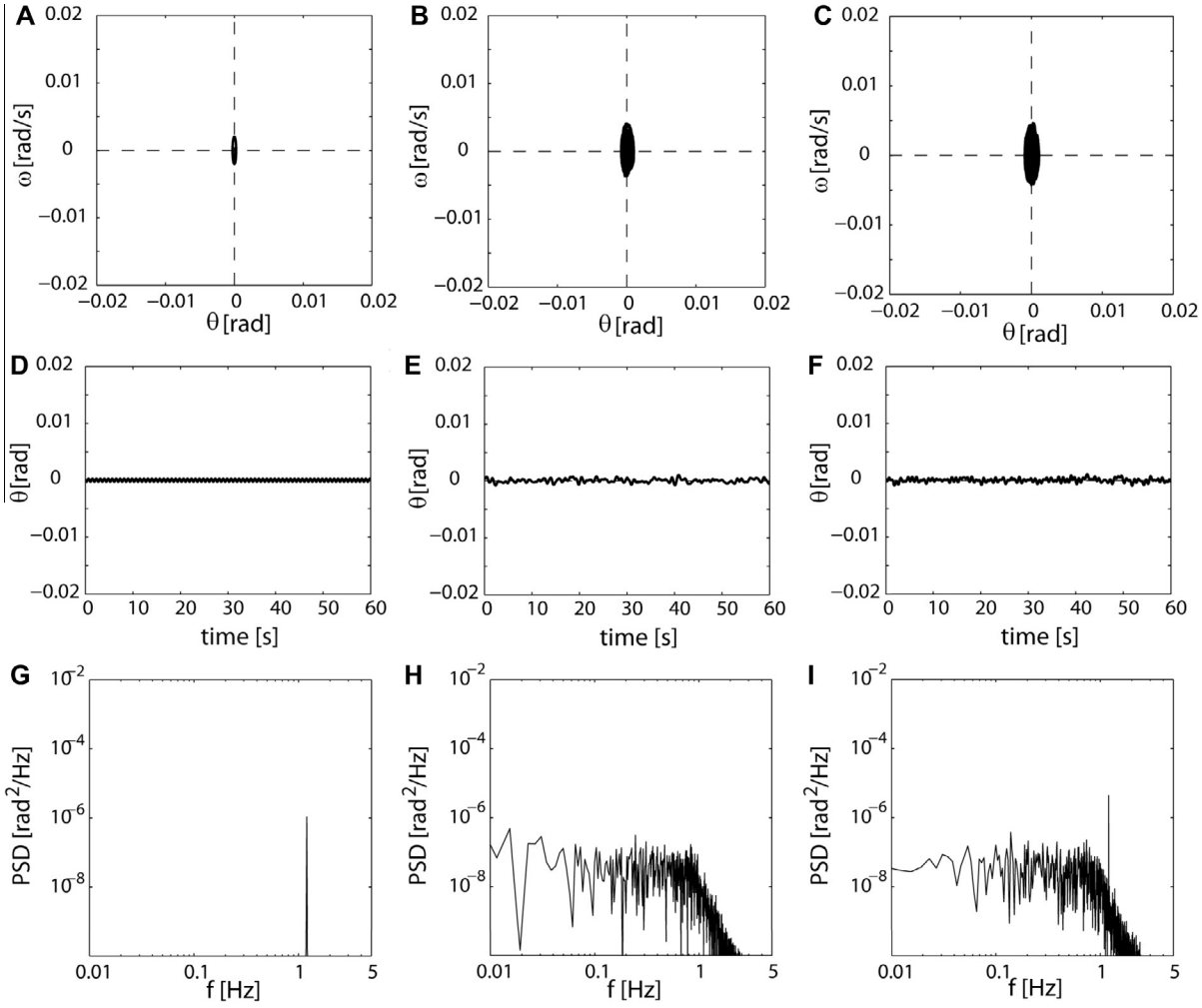

Fig. 2. Typical dynamics of the continuous control model with endogenous disturbance torque. See Fig. 1A for the corresponding dynamics without the disturbance torque. A, D and G: Postural sway only with the periodic disturbance $T_{\text{dist}}^{\text{per}}$. B, E and F: Postural sway only with the small noisy disturbance $T_{\text{dist}}^{\text{noise}}$. C, F and I: Postural sway with the periodic hemodynamic perturbation $T_{\text{dist}}^{\text{hemo}}$. For each triplet, top, middle and bottom panels are the steady-state trajectory on the θ-ω plane, the waveform of θ and the PSD, respectively.

which is about 1.0 Hz for the parameter values that we use. In this way, the continuous control model with the typical feedback gain parameters hardly exhibits the human-like sway pattern with the power law behavior at the low frequency band.

3.1.2. Dynamics of the intermittent model for small $|a|$ with disturbance

The intermittent control model with the typical values of the active feedback gains exhibits sway dynamics with much larger amplitude than that in the continuous control model for any of $T_{\text{dist}}^{\text{per}}$, $T_{\text{dist}}^{\text{noise}}$ and $T_{\text{dist}}^{\text{hemo}}$ (Figs. 3 and 4). This suggests that the upright posture in the intermittent control model is not rigidly fixed, but flexible. As we observed for the noise-less model, sway dynamics of the intermittent model changes depending on the parameter value of a. Figs. 3 and 4 show the forced dynamics of the intermittent control model for $a = -0.3$ and $a = -0.989$, respectively, corresponding to the noise-less limit cycle dynamics in Figs. 1B and 1C.

In Figs. 3A, D and G for the intermittent control model with $a = -0.3$, the pendulum is forced only by the periodic perturbation $T_{\text{dist}}^{\text{per}}$. The parameter value of a is small (i.e., $|a|$ is small), by which the slope of the boundary line is less steep. In this case, the pendulum's motion is entrained by the periodic perturbation. It shows a periodic oscillation with the period of about 4.2 s ($\sim$ 0.24 Hz) that includes five sinusoidal hemodynamic cycles, corresponding to a 5-periodic point of the Poincaré map F defined by Eq. (13). Amplitude and location of the forced limit cycle in the θ-ω plane are roughly the same as those of the original unforced limit cycle shown in Fig. 1B. The limit cycle trajectory does not go beyond the stable and the unstable manifolds, leading to the motion of the pendulum's state restricted in the right-hand-side of the θ-ω plane. Note that, depending on the initial condition, the steady-state limit cycle can be located in the left-side of the plane, because of the bistability of the model's dynamics. Periodicity of the dynamics results in the PSD with several sharp peaks including a peak at the base cycle.

When the pendulum is perturbed only by the small white noise $T_{\text{dist}}^{\text{noise}}$, the unforced limit cycle in Fig. 1B is randomly distorted (Figs. 3B and E). Amplitude and cycle length of the randomly modulated oscillation vary, because the pendulum's state kicked far away from the unforced limit cycle by the noise moves around the unforced limit cycle with a large amplitude and a long cycle length, whereas that kicked near the switching boundary experiences chattering-like repeated switchings between the on-region and the off-region with small amplitude and cycle length that is shorter than the period of the unforced limit cycle. For the mechanism of sliding motion along the boundary line with the chattering-like behavior, see [19,10,5]. Because of the variation of amplitude and cycle length, PSD of the sway exhibits the power law scaling at the low frequency band 0.1–0.7 Hz (Fig. 3H). Dynam-

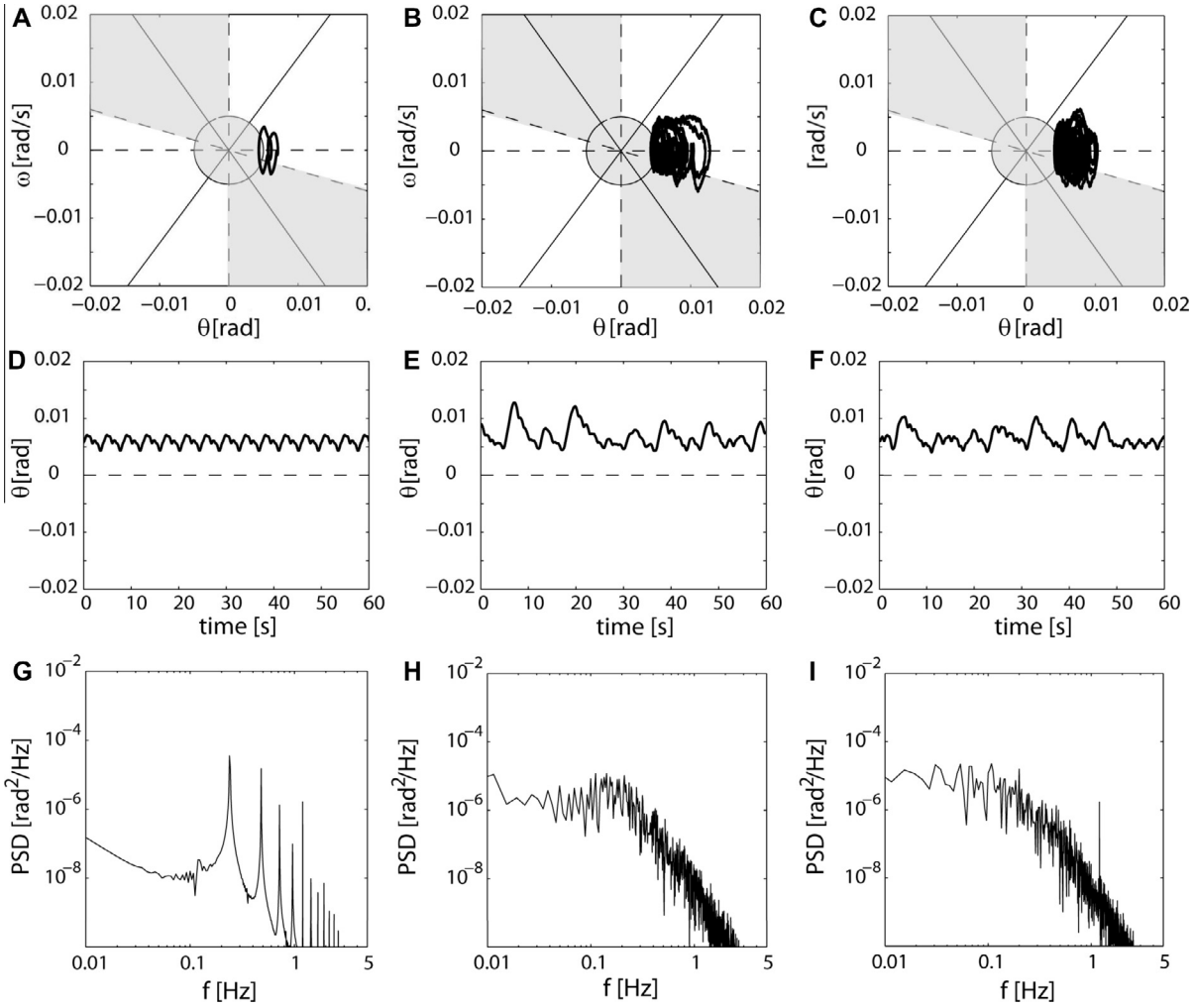

Fig. 3. Typical dynamics of the intermittent control model with $a = -0.3$ in response to endogenous disturbance torque. See Fig. 1B for the corresponding dynamics without the disturbance torque. See legend of Fig. 2 for configuration of the panels.

ics of the intermittent control model with $a = -0.3$ forced by the sum of periodic and random components of the hemodynamic perturbation $T_{\text{dist}}^{\text{hemo}}$ is almost the same as that of the model forced by the random perturbation alone (Figs. 3).

3.1.3. Dynamics of the intermittent model for large |a| with disturbance

For large parameter values of a, the switching boundary line becomes steep and close to the stable manifold whose slope is determined by Eq. (5). As in Figs. 4G for $a = -0.989$, the intermittent control model forced only by the periodic component of the hemodynamic perturbation $T_{\text{dist}}^{\text{per}}$ shows a chaotic oscillation of large amplitude.

Different from the case of small value of a shown in Fig. 3A, the trajectory of the model runs across the stable manifold and moves into the left-hand-side of the θ-ω plane where the other bistable, unforced limit cycle is located. This is because the pendulum's state can go easily beyond the boundary line that is close to the stable manifold along which the unforced limit cycle is formed. In a similar way, the pendulum's state moves back and forth between the bistable unforced limit cycles located at the left and the right half planes. The chaotic oscillation includes a variety of amplitudes and cycle lengths, resulting in the long-term-correlated power law behavior at the low frequency band of the PSD (Fig. 4G) only by the small periodic perturbation.

The random perturbation $T_{\text{dist}}^{\text{noise}}$ also causes a hopping behavior between the bistable unforced limit cycles as in the chaotic dynamics for the periodically forced intermittent control model (Figs. 4B and E). Variation of the long-term correlated chaotic oscillation increases when the model is disturbed by the sum of the periodic and the random perturbations (Figs. 4C and F). These dynamics in both cases lead to the power law behavior in the PSD at the low frequency band (Figs. 4H and I).

3.2. Bifurcation diagrams with corresponding Lyapunov exponent and PSD

Fig. 5 shows the bifurcation diagrams, with the corresponding changes in the PSD, the scaling exponent β, and the largest Lyapunov exponent, as the parameter value of a changes for the intermittent control model with and without the periodic forcing for $\sigma = 0$ Nm and $\sigma = 0.09$ Nm.

The bifurcation diagram of the intermittent control model with no disturbance shows a sequence of bifurcations, including period-halving bifurcations as the value of $|a|$ increases (Fig. 5A). We can see from the diagram that the intermittent control model is stable in the range of $|a|$ about [0.15,1.3], otherwise unstable. In particular, the model shows chaotic dynamics for several intervals of $|a|$ within [0.15,0.35] for which the largest Lyapunov exponent is positive, except for some small periodic windows (Fig. 5C). For the

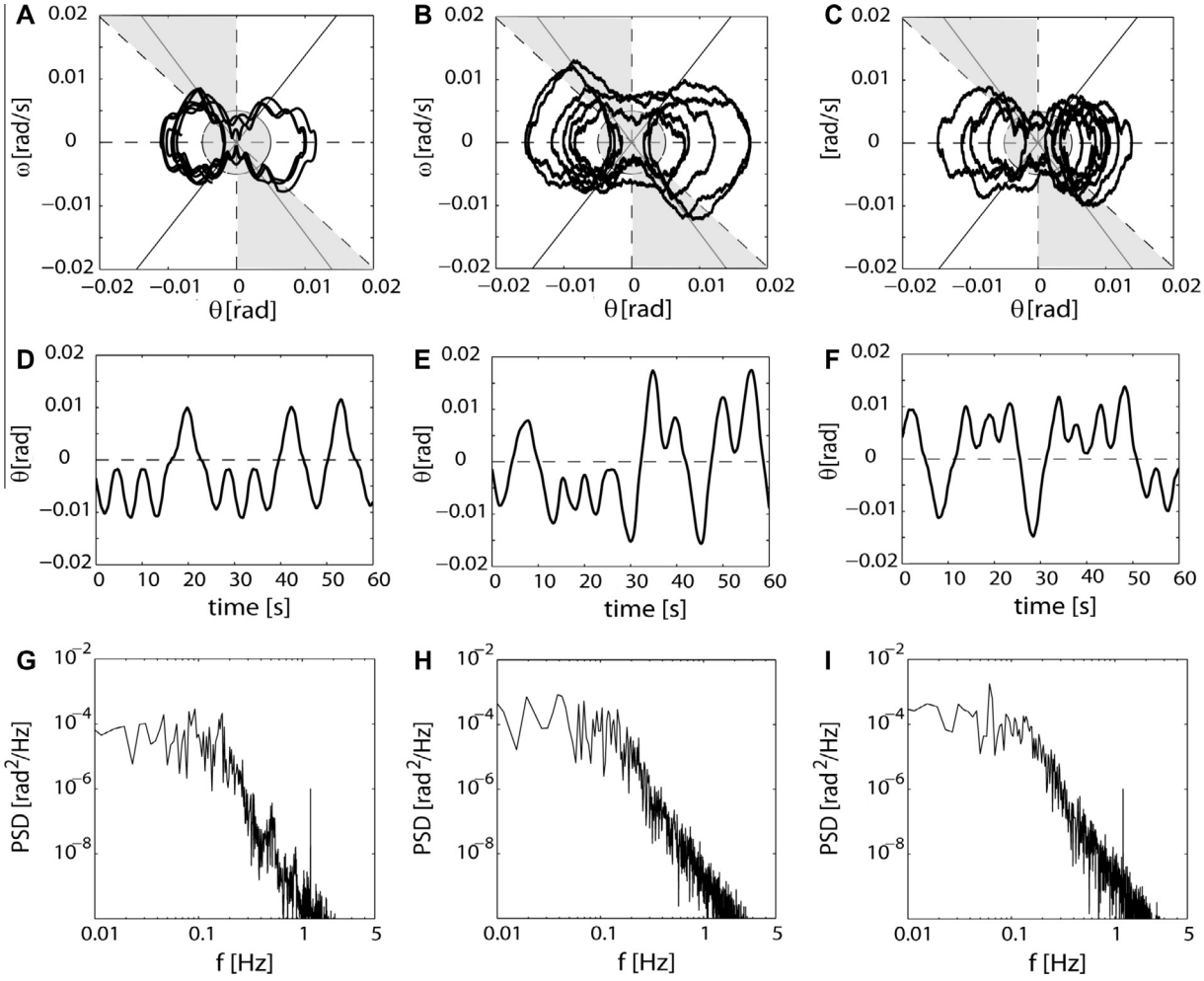

Fig. 4. Typical dynamics of the intermittent control model with $a = -0.989$ in response to endogenous disturbance torque. See Fig. 1C for the corresponding dynamics without the disturbance torque. See legend of Fig. 2 for configuration of the panels.

remaining intervals, the model's dynamics is periodic mostly with period 2 or 3. Fig. 5I represents the corresponding changes in the shape of PSD. One can observe that the PSD exhibits the power law behavior at the low frequency range when the model's dynamics is chaotic, where the scaling exponent β at the low frequency band (0.1–0.7 Hz) is close to 1.5, corresponding to the Hurst exponent H close to 1/4 as reported in the experimental study [11].

When the intermittent control model is forced by the periodic perturbation, the bifurcation diagram becomes complicated, which includes wider ranges of $|a|$ exhibiting chaotic dynamics (Figs. 5B and D). In particular, the model's dynamics is typically chaotic for most large values of $|a|$, roughly in the range of [0.95,1.2]. For this parameter range, chaotic sequences of stroboscopically observed states distribute in a wide range of tilting angle, implying that the pendulum's state moves back and forth chaotically between the left and the right half planes as in Fig. 4A. PSDs of these chaotic postural sway exhibit the power law behavior at the low frequency band (Fig. 5J).

Figs. 5E and F represent the stochastic bifurcation diagrams, corresponding to the deterministic diagrams in Figs. 5A and B, respectively. Overall shape of each stochastic bifurcation diagram is influenced by the corresponding deterministic bifurcation structure. The small stochastic disturbance mostly drowns out the chaotic behavior. However, the largest Lyapunov exponent exhibits slightly positive values for $|a|$ around 0.7 and 1.2 (Figs. 5G and H), suggesting that noisy sway dynamics of the model could be weakly chaotic even with the small stochastic disturbance.

Although the probabilistic distribution of the pendulum's state is more clearly separated into positive (right-half of the θ-ω plane) and negative (left-half of the θ-ω plane) tilt angles in Fig. 5E than that in Fig. 5F, one can observe that amplitude of the sway oscillation varies widely. This observation suggests that the corresponding cycle length of the stochastic oscillation also varies widely, leading to the PSD with the power law behavior at the low frequency band for each of the models forced by the random perturbation only (Figs. 5M) and by the noisy periodic perturbation (Figs. 5L and N). The scaling factor β at the low frequency band (0.1–0.7 Hz) is close to 1.5 when $|a|$ is small. The value of β increases almost monotonically as the value of $|a|$ increases.

4. Discussion

In this study, we considered postural sway dynamics of an inverted pendulum model with an intermittent, as well as the traditional continuous feedback control strategies. We hypothesized that the almost periodic hemodynamic torque perturbation of amplitude 0.4 Nm to the ankle joint could be the major source of endogenous perturbation inducing the human postural sway during quiet standing. The small amplitude of the perturbation was specified according to the experimental observation by [1]. We then examined whether each control model could exhibit

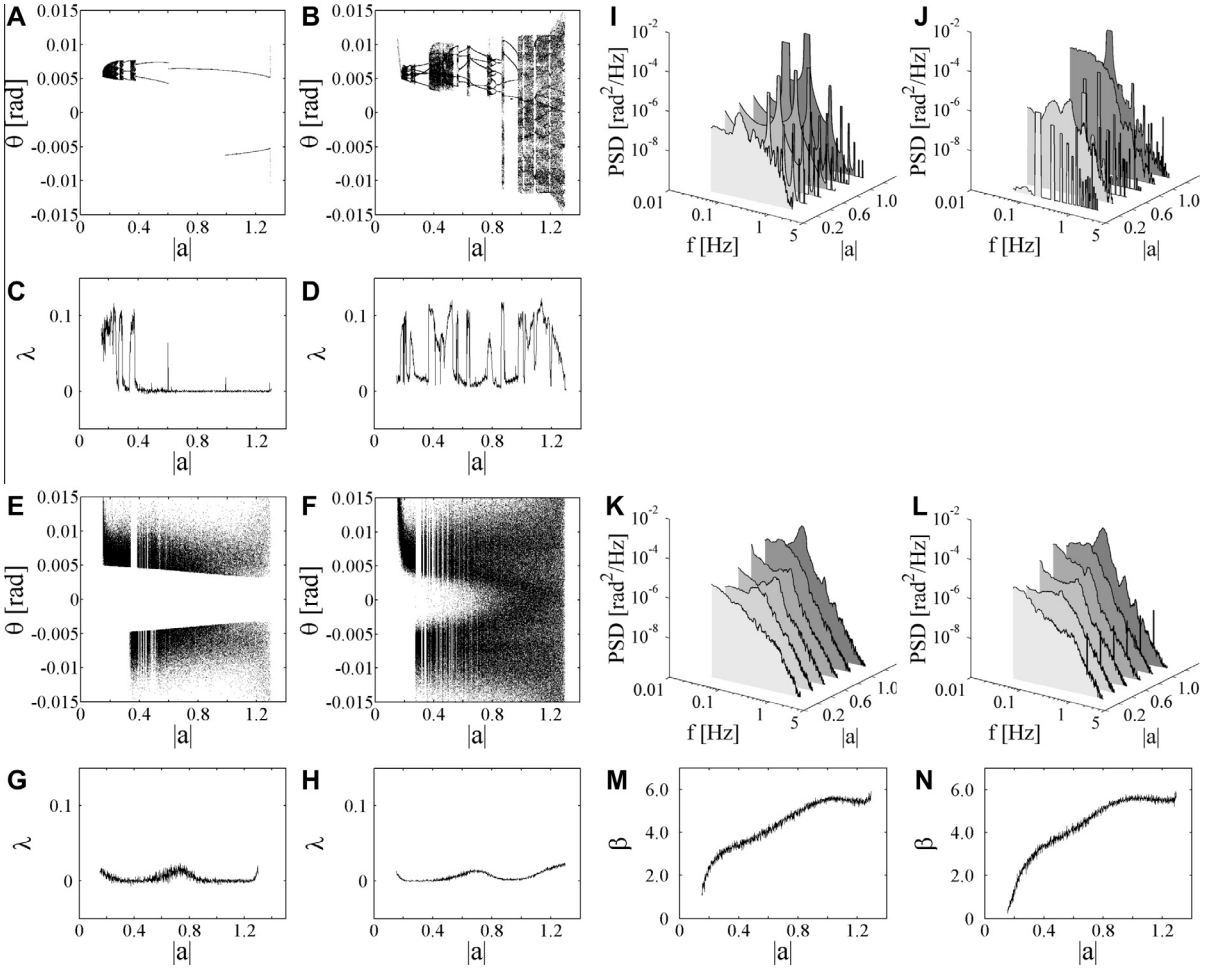

Fig. 5. Bifurcations diagrams with corresponding changes in the PSD, the scaling factor β, and the largest Lyapunov exponent λ in the intermittent control model as the function of the absolute value of the parameter a. A: Bifurcation diagram of the model with no disturbance based on the Poincaré map G defined by Eq. (14), with the corresponding Lyapunov exponent λ in C. B: Bifurcation diagram of the model with the periodic perturbation $T_{\text{dist}}^{\text{per}}$ based on the Poincaré map F defined by Eq. (13), with the corresponding Lyapunov exponent λ in D. E and F: Bifurcation diagrams when the small random perturbation ($\sigma = 0.09$ Nm) is added, namely, with $T_{\text{dist}}^{\text{noise}}$ in E and with $T_{\text{dist}}^{\text{hemo}}$ in F. G and H: Changes in the Lyapunov exponent corresponding to E and F, respectively. I and J: PSDs as $|a|$ changes, corresponding to A and B, respectively. K and L: PSDs as $|a|$ changes, corresponding to E and F, respectively. M and N: Changes in the scaling exponent β as $|a|$ changes, corresponding to K and L, respectively. For each bifurcation diagram, only stable dynamics obtained from a single initial condition were plotted. Thus, the diagram does not explain bistability of the intermittent control model.

human-like postural sway when it was weakly perturbed by periodic and/or random forcing mimicking the hemodynamic perturbation. Based on the power law behavior in the power spectral density (PSD) at the low frequency band 0.1–0.7 Hz for the human postural sway [11], we showed that the continuous control model with typical feedback gain parameters hardly exhibited the human-like sway pattern, while the intermittent control model did.

How can the intermittent control model exhibit the human-like postural sway pattern? There are two reasons for this. The first one is flexibility of the upright equilibrium in the intermittent control model. The second is the slow dynamics of the saddle-type vector field along with the stable and unstable manifolds that governs the model's behavior intermittently. Origins of the flexible human postural balancing include small passive stiffness of the ankle joint insufficient for stabilizing the upright stance [2,4,31] and the paradoxical non-spring-like property of calf muscle with compliant Achilles tendon during quiet stance [3]. Although both the continuous and the intermittent control models assumed physiologically plausible small passive gains of K and B, the feedback gains of the intermittent active controller when it was turned on, which also contributes to the ankle stiffness during standing, were much smaller than those of the continuous controller. Moreover, when active control was turned off in the intermittent control model, the active gains were zero. The compliant ankle joint provided by the small passive and active gains in the intermittent control model allowed the small hemodynamic perturbation to induce the postural sway with relatively large amplitude.

In this study, we modeled the random torque noise using a Gaussian white noise of tiny amplitude as the residual error from the periodic component of the hemodynamic perturbation. The use of white noise of tiny amplitude ($\sigma = 0.09$ Nm) for simulating stochastic postural sway is not common. Most of the previous studies modeling human postural sway have been assuming colored torque noise of large amplitude [14,17,32]. This might be because 1) the additive Gaussian white noise driving the continuous control model cannot exhibit the power law behavior at the low frequency band 0.1–0.7 Hz as shown in this study, and 2) the small intensity of noise, such as used in this study, applied to the continuous control model cannot induce the postural sway of the relatively large amplitude about 0.01–0.02 m. Indeed, Maurer et al. [14] assumed the first order low-pass filtered colored torque noise that disturbs the continuous control model. They assumed the filter with the time constant of 100 s and the corner frequency of 0.01 Hz, and the noise amplitude of about 450 Nm, which is enormously too large and thus physiologically implausible as pointed out in [19]. In this way, the power-law-like behavior in the PSD at the low frequency band in the continuous control model was dominated by this huge colored noise.

We showed that the mechanism underlying the power law behavior at 0.1–0.7 Hz in the intermittent control model was completely different from that in the continuous control model. The noise-less periodic hemodynamic forcing could even exhibit the power law behavior at the low frequency band if the switching boundary (the parameter value of a) was appropriately tuned for chaotic dynamics. In this regard, it is interesting to mention that there are several studies reporting a chaotic nature of human postural sway [33,34], in contradiction to most of the studies concluded that the postural sway is a purely stochastic process [11]. See discussion in [35,36]. We showed that the Gaussian white noise with physiologically plausible and experimentally obtained amplitude enhanced the power law behavior for the wide range of the a-value, making the power law behavior robust against variation of the a-value. The origin of the power law behavior in the intermittent control model was the varied cycle length of the oscillation, which was determined by the distance between the state of the pendulum when the active control torque was switched off and the stable manifold of the non-actively-actuated pendulum. The smaller the distance, the longer was the cycle length of the oscillation.

There might be other mechanisms that can generate the postural sway exhibiting the power law behavior at the low frequency band [22]. Multiplicative noise that alters the proportional feedback gain (P) in a noisy manner could be one of the alternative mechanisms, where the system is tuned near the edge of stability and a critical control parameter is stochastically forced back and forth across the boundary [37]. In order to better understand the control strategy of central nervous system for stabilizing the upright posture, we further need to consider robustness of hypothesized strategies and generalization of the strategies to more physiologically detailed multi-joint inverted pendulum [38,39].

It is interesting to note that the postural sway pattern, including the scaling exponent of the power law behavior at the low frequency band, shows individual and age dependencies [40]. Moreover, neurological diseases such as Parkinson's disease also cause variations of the exponent [41,42]. Changes in the scaling exponent at the low frequency band as the function of parameter value of a examined in this study could be useful to better characterize ability of posture control.

In conclusion, the results of this study suggest that deterministic, including chaotic, slow oscillations that characterize the intermittent control strategy, together with the small hemodynamic perturbation, could be a possible mechanism for generating the postural sway.

Acknowledgments

This work was supported in part by JSPS grants-in-aid 21-416 and 23300166, E.U. grant HUMOUR (FP7-ICT-231724), MEXT HPCI strategic program (Theme 3), and the Mitsubishi Foundation.

References

[1] S. Conforto, M. Schmid, V. Camomilla, T. D'Alessio, A. Cappozzo, Hemodynamics as a possible internal mechanical disturbance to balance, Gait and Posture 14 (1) (2001) 28.
[2] P. Morasso, V. Sanguineti, Ankle muscle stiffness alone cannot stabilize balance during quiet standing, Journal of Neurophysiology 88 (4) (2002) 2157.
[3] I. Loram, C. Maganaris, M. Lakie, Paradoxical muscle movement in human standing, Journal of Physiology 556 (3) (2004) 683.
[4] M. Casadio, P. Morasso, V. Sanguineti, Direct measurement of ankle stiffness during quiet standing: Implications for control modeling and clinical application, Gait and Posture 21 (4) (2005) 410.
[5] Y. Asai, Y. Tasaka, K. Nomura, T. Nomura, M. Casadio, P. Morasso, A model of postural control in quiet standing: robust compensation of delay-induced instability using intermittent activation of feedback control, PLoS ONE 4 (7) (2009). art. no. e6169.
[6] T. Prieto, J. Myklebust, R. Hoffmann, E. Lovett, B. Myklebust, Measures of postural steadiness: differences between healthy young and elderly adults, IEEE Transactions on Biomedical Engineering 43 (9) (1996) 956.
[7] K. Nomura, K. Fukada, T. Azuma, T. Hamasaki, S. Sakoda, T. Nomura, A quantitative characterization of postural sway during human quiet standing using a thin pressure distribution measurement system, Gait and Posture 29 (4) (2009) 654.
[8] M. Schmid, S. Conforto, D. Bibbo, T. D'Alessio, Respiration and postural sway: detection of phase synchronizations and interactions, Human Movement Science 23 (2) (2004) 105.
[9] H. Van Der Kooij, R. Jacobs, B. Koopman, F. Van Der Helm, An adaptive model of sensory integration in a dynamic environment applied to human stance control, Biological Cybernetics 84 (2) (2001) 103.
[10] A. Bottaro, Y. Yasutake, T. Nomura, M. Casadio, P. Morasso, Bounded stability of the quiet standing posture: an intermittent control model, Human Movement Science 27 (3) (2008) 473.
[11] J. Collins, C. De Luca, Random walking during quiet standing, Physical Review Letters 73 (5) (1994) 764.
[12] H. Van Der Kooij, E. Van Asseldonk, F. Van Der Helm, Comparison of different methods to identify and quantify balance control, Journal of Neuroscience Methods 145 (1–2) (2005) 175.
[13] G Rangarajan, M. Ding, Integrated approach to the assessment of long range correlation in time series data, Physical Review E – Statistical Physics, Plasmas, Fluids, and Related Interdisciplinary Topics 61 (5A) (2000) 4991–5001.
[14] C. Maurer, R. Peterka, A new interpretation of spontaneous sway measures based on a simple model of human postural control, Journal of Neurophysiology 93 (1) (2005) 189.
[15] K. Masani, M. Popovic, K. Nakazawa, M. Kouzaki, D. Nozaki, Importance of body sway velocity information in controlling ankle extensor activities during quiet stance, Journal of Neurophysiology 90 (6) (2003) 3774.
[16] H. Van Der Kooij, E. De Vlugt, Postural responses evoked by platform pertubations are dominated by continuous feedback, Journal of Neurophysiology 98 (2) (2007) 730.
[17] A. Vette, K. Masani, K. Nakazawa, M. Popovic, Neural-mechanical feedback control scheme generates physiological ankle torque fluctuation during quiet stance, IEEE Transactions on Neural Systems and Rehabilitation Engineering 18 (1) (2010) 86.
[18] T. Kiemel, Y. Zhang, J. Jeka, Identification of neural feedback for upright stance in humans: stabilization rather than sway minimization, Journal of Neuroscience 31 (42) (2011) 15144.
[19] A. Bottaro, M. Casadio, P. Morasso, V. Sanguineti, Body sway during quiet standing: is it the residual chattering of an intermittent stabilization process?, Human Movement Science 24 (4) (2005) 588
[20] J. Collins, C. De Luca, Open-loop and closed-loop control of posture: a random-walk analysis of center-of-pressure trajectories, Experimental Brain Research 95 (2) (1993) 308.
[21] C. Eurich, J. Milton, Noise-induced transitions in human postural sway, Physical Review E – Statistical Physics, Plasmas, Fluids, and Related Interdisciplinary Topics 54 (6) (1996) 6681.
[22] J. Milton, J. Townsend, M. King, T. Ohira, Balancing with positive feedback: the case for discontinuous control, Philosophical Transactions of the Royal Society A: Mathematical, Physical and Engineering Sciences 367 (1891) (2009) 1181.
[23] T. Insperger, G. Stepan, On the dimension reduction of systems with feedback delay by act-and-wait control, IMA Journal of Mathematical Control and Information 27 (4) (2010) 457.
[24] I. Loram, H. Gollee, M. Lakie, P. Gawthrop, Human control of an inverted pendulum: is continuous control necessary? is intermittent control effective? is intermittent control physiological?, Journal of Physiology 589 (2) (2011) 307
[25] P. Gawthrop, I. Loram, M. Lakie, H. Gollee, Intermittent control: a computational theory of human control, Biological Cybernetics 104 (1–2) (2011) 31.
[26] R. Peterka, Sensorimotor integration in human postural control, Journal of Neurophysiology 88 (3) (2002) 1097.
[27] T. Tateno, S. Doi, S. Sato, L. Ricciardi, Stochastic phase lockings in a relaxation oscillator forced by a periodic input with additive noise: a first-passage-time approach, Journal of Statistical Physics 78 (3–4) (1995) 917.
[28] S. Doi, J. Inoue, S. Kumagai, Spectral analysis of stochastic phase lockings and stochastic bifurcations in the sinusoidally forced van der pol oscillator with additive noise, Journal of Statistical Physics 90 (5–6) (1998) 1107.
[29] M. Rosenstein, J. Collins, C. De Luca, A practical method for calculating largest lyapunov exponents from small data sets, Physica D: Nonlinear Phenomena 65 (1–2) (1993) 117.
[30] R. Hegger, H. Kantz, T. Schreiber, Practical implementation of nonlinear time series methods: The tisean package, Chaos 9 (2) (1999) 413.
[31] I. Loram, M. Lakie, Direct measurement of human ankle stiffness during quiet standing: The intrinsic mechanical stiffness is insufficient for stability, Journal of Physiology 545 (3) (2002) 1041.
[32] C. Chow, J. Collins, Pinned polymer model of posture control, Physical Review E 52 (1) (1995) 907.
[33] N. Yamada, Chaotic swaying of the upright posture, Human Movement Science 14 (6) (1995) 711.
[34] H. Ghomashchi, A. Esteki, J. Sprott, A. Nasrabadi, Identification of dynamic patterns of body sway during quiet standing: is it a nonlinear process?, International Journal of Bifurcation and Chaos 20 (4) (2010) 1269
[35] T. Kiemel, K. Oie, J. Jeka, Multisensory fusion and the stochastic structure of postural sway, Biological Cybernetics 87 (4) (2002) 262.
[36] M. Roerdink, M. De Haart, A. Daffertshofer, S. Donker, A. Geurts, P. Beek, Dynamical structure of center-of-pressure trajectories in patients recovering from stroke, Experimental Brain Research 174 (2) (2006) 256.

[37] J. Cabrera, J. Milton, On-off intermittency in a human balancing task, Physical Review Letters 89 (15) (2002) 158702/1–158702/4.
[38] Y. Suzuki, T. Nomura, P. Morasso, Stability of a double inverted pendulum model during human quiet stance with continuous delay feedback control, in: Annual International Conference of the IEEE Engineering in Medicine and Biology Society, Conference 2011, IEEE Engineering in Medicine and Biology Society, 2011, pp. 7450–7453.
[39] Y. Suzuki, T. Nomura, M. Casadio, P. Morasso, Intermittent control with ankle, hip, and mixed strategies during quiet standing: a theoretical proposal based on a double inverted pendulum model, Journal of Theoretical Biology 310 (2012) 55.
[40] J. Kim, Y. Kwon, G.-M. Eom, J.-H. Jun, J.-W. Lee, G.-R. Tack, Effects of vision, age and gender on structural and global posturographic features during quiet standing, International Journal of Precision Engineering and Manufacturing 13 (6) (2012) 969.
[41] C. Maurer, T. Mergner, R. Peterka, Abnormal resonance behavior of the postural control loop in parkinson's disease, Experimental Brain Research 157 (3) (2004) 369.
[42] T. Yamamoto, Y. Suzuki, K. Nomura, T. Nomura, T. Tanahashi, K. Fukada, T. Endo, S. Sakoda, A classification of postural sway patterns during upright stance in healthy adults and patients with parkinson's disease, Journal of Advanced Computational Intelligence and Intelligent Informatics 15 (8) (2011) 997.